Food Hydrocolloids 136 (2023) 108280

Contents lists available at ScienceDirect

Food Hydrocolloids

journal homepage: www.elsevier.com/locate/foodhyd

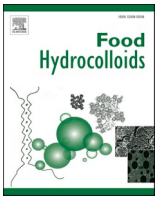

Dual complexation using heat moisture treatment and pre-gelatinization to enhance Starch–Phenolic complex and control digestibility

Patarawadee Sudlapa, Prisana Suwannaporn *

Department of Food Science and Technology, Faculty of Agro-Industry, Kasetsart University, Bangkok, 10900, Thailand

ARTICLE INFO

Keywords:
Dual complexation
Starch–phenol complex
V-amylose
Digestibility
Riceberry

ABSTRACT

Phenol is a competitive inhibitor for digestive enzymes, moreover, it can form complexes with starch either inclusion (V-type) or non-inclusion. These complexes can resist enzymatic digestion and are considered as RS type 5. However, phenol is usually bulky and does not easily enter the amylose helix cavity. The dual starch–-phenolic complexation was proposed to increase single helix using heat moisture treatment (HMT) altogether with pre-gelatinization. The dual complexation of rice starch and Riceberry extract (HMT-RSP-Riceberry) exhibited the highest V-amylose and % crystallinity (30.8%, 31.5%) compared with native starch (14.5%, 19.8%). The high total phenolic and hydroxycinnamic acid content especially ferulic acid in Riceberry extract were effectively inhibited α-amylase activity. The complexing index of HMT-RSP-Riceberry was double (10.2%) the conventional process (5.1%). The single helix fraction which promote loose structure, allowing more phenol to move inside and between the helix cavities, increased noticeably in the HMT-RSP-Riceberry (30.7%) compared with native starch (4.3%). HMT-RSP-Riceberry had lower RDS but higher SDS and RS (77.2%, 7.1%, 15.8%) than conventional process using 15% gallic acid (positive control) (87.6, 5.3, and 7.1%), and native starch (negative control) (95.9, 1.5, 2.6%, respectively). The dual complexation process was more applicable in terms of reasonable amount of phenol used, no undesirable taste, and no chemical used during process. This physically modified inclusion complexes could improve starch digestibility with potential application in healthy foods.

1. Introduction

Rice has a high glycemic index (GI), especially after cooking, which has led to its reduced consumption. Attempts to reduce rice GI include parboiling or rice breeding program. Phenolic compounds act as competitive inhibitors of digestive enzymes (Sun, Warren, & Gidley, 2019). This inhibitory activity is caused by hydrogen bonding between the aromatic ring of phenolic compounds and tryptophan residue of α-amylase (Kwon et al., 2007). Hydroxycinnamic acid had a C═C double bond, which formed a highly conjugated system with the carbonyl group; hence stabilized the binding forces at the enzyme's active site, resulting in an inhibition of α-amylase (Sun et al., 2019). Phenol and starch can form two types of complexes: inclusion (V-type) and non-inclusion complexes (Zhu, 2015). The formation of the V type inclusion complex was based on the hydrophobic interaction within the cavity of the single helix of amylose with small guest molecules, such as phenol, lipid, iodine, etc. (Obiro, Sinha, & Emmambux, 2012). The amylose–phenol inclusion complexes showed a V-type structure decreased starch granule swelling and formed a denser starch network, which limited enzyme accessibility. This starch is usually defined as resistant-starch type 5 (RS 5), which was not absorbed in the small intestine but could be fermented in the large intestine. RS 5 was reported to considerably reduce GI, positively impacting the blood glucose level. However, this complex could be achieved with high phenol concentration because of its bulky size, making it impossible to enter the amylose helix cavity. Furthermore, an excessive amount of phenol was used to obtain desirable complexation. Gallic acid is commonly used in many studies and was applied at approximately 30%–50% by starch weight (Chen et al., 2006; Chi et al., 2018, 2019; Han, Bao, Wu, & Ouyang, 2020; Li, Yao, Du, Deng, & Li, 2018; Liu, Chen, Xu, Liang, & Zheng, 2019). This attempt was not applicable due to the high cost of excessive phenol and unacceptable consumer taste, as gallic acid has an unfavorable bitter/astringent taste. Rice bran, an abundant byproduct from rice milling, and milky-stage rice were reported to have high total phenol and hydroxycinnamic acid. Hydroxycinnamic acids found in rice include ferulic, *p*-coumaric, caffeic, and sinapic acids, which efficiently

* Corresponding author.
E-mail address: prisana.s@ku.th (P. Suwannaporn).

https://doi.org/10.1016/j.foodhyd.2022.108280
Received 22 February 2022; Received in revised form 6 October 2022; Accepted 29 October 2022
Available online 1 November 2022

form a complex with starch (Ratseewo, Warren, & Siriamornpun, 2019; Sun et al., 2019).

Starch–phenolic inclusion processes were applied either with physical, chemical, or enzymatic methods. Physical modification included pre-gelatinization and non-thermal processing, such as high hydrostatic pressure (Guo, Zhao, Chen, Chen, & Zheng, 2019), ultrasound (Zhao et al., 2019; Zhao, Wang, Zheng, Chen, & Guo, 2019), microwave (Zhao et al., 2019), high-speed shear, high-pressure homogenization (Chi et al., 2019; Zhao et al., 2019), and plasma (Gao et al., 2021) (Table 1). Pre-gelatinization was an easy and common method for complexing starch and phenol. This process caused the starch granules to be destroyed, thereby increasing amylose leaching to form phenolic complexes. During cooling, phenol was trapped in the starch structure either by inclusion or non-inclusion. However, the inclusion efficiency of this method was quite low (Han et al., 2020). There were attempts to force the phenol into the helices by combining pre-gelatinization with ultrahigh-pressure (100–600 MPa), high-speed shear (6000 rpm), or high-pressure homogenizer (150 MPa) (Chi et al., 2019; Liu et al., 2019). This molecular rearrangement, as well as the competitive inhibition of phenol itself, were then used to control starch digestibility (Wang, Gao, Liu, Zhang, & Guo, 2016).

In this study, the dual starch–phenolic complexation using a combined method of heat moisture treatment (HMT) and pre-gelatinization was proposed to increase complexation efficiency. HMT was reported to be able to increase single helix of amylose, loosen the tight double helices structure, which ease phenol to enter the single amylose cavity or trapped between amylose chains. This inclusion process was proposed to accelerate complex forming either by inclusion (V-type) or non-inclusion. Moreover, the crude phenolic extracts from rice brans of Riceberry, Jasmin rice, and milky stage rice were used to study the effect of total phenolic content and hydroxycinnamic acid on complexation and starch digestibility. Milky stage rice was interested as it was reported to have high phenolics, flavonoids, and ferulic than mature rice (Pantoa et al., 2020).

2. Materials and methods

2.1. Starch isolation

High amylose rice (Chainat 1 variety, Watcharawan Green Farm, Phayao, Thailand) (apparent amylose content 25–27%) was soaked in water for 12 h and milled using super mass colloider (MK PB6-2, Masuko Sangyo, Saitama, Japan). The slurry was centrifuged using a basket centrifuge (CE-03, Thai-Wasino Electric, Samutprakarn, Thailand). The precipitate was extracted for starch by soaking with 0.1 M NaOH with stirring for 3 h and centrifuged (3,000×*g*) for 10 min. The precipitate was soaked again with 0.1 M NaOH with stirring for 1 h and centrifuged. The yellow layer on the precipitate's surface was scraped out and the white starch layer was washed with distilled water and centrifuged five times. The final starch solution was neutralized with 1 M HCl, dried at 40 °C until moisture content reached 10%–12%, passed through a 100-mesh sieve, and stored at 4 °C in a sealed plastic bag.

2.2. Crude phenolic extraction

Rice bran of colored rice (Riceberry variety), white rice (KDML 105, or Jasmine rice), and milky stage rice (Riceberry variety) (Watcharawan Green Farm, Phayao, Thailand) were selected as phenol sources, accounting for the hydroxycinnamic acid content. Crude phenol was extracted using 80% methanol at a ratio of sample:solvent (1:5 w/v), stirred at 30 °C for 2 h, and centrifuged (3000 g) for 10 min. The residue was re-extracted under the same condition and the supernatant was combined. The solvent was removed using a rotary vacuum evaporator (R152, Buchi, Flawil, Switzerland) at 40 °C. The concentrate slurry was lyophilized and stored at −20 °C (Butsat & Siriamornpun, 2010).

2.3. Total phenolic content

The total phenolic content was determined using the Folin–Ciocalteu method (Liu & Yao, 2007). Briefly, the extract solution (0.4 mL) was shaken for 1 min with diluted (1:10 with water) Folin–Ciocalteu reagent (Merck, Darmstadt, Germany) (2 mL). After that, 5% Na_2CO_3 (1.6 mL) was added and kept in a dark place at room temperature for 30 min. The absorbance was measured at 760 nm using a UV–Vis spectrophotometer (Genesys 10S, Thermo Fisher Scientific, MA, USA). The phenolic content was determined using gallic acid (GK7318, Glentham Life Sciences, Corsham, UK) as a standard.

2.4. Characterization of phenolic acid using HPLC

Crude phenolic solution (20 μL) was fractionated using HPLC (LC-10A series HPLC, Shimadzu, Kyoto, Japan) equipped with a diode array detector and Inertsil C18 analytical column (250 × 4.6 mm, 5 μm). The mobile phase consisted of purified water and phosphoric acid at pH 2.58 (solvent A) and acetonitrile (solvent B) at a 0.8 mL/min flow rate. Gradient elution was from 0 to 5 min (linear gradient from 5% to 9% solvent B), 5–15 min (9% solvent B), 15–22 min (linear gradient from 9% to 11% solvent B), 22–38 min (linear gradient from 11% to 18% solvent B), 38–43 min (18%–23% solvent B), 43–44 min (23%–90% solvent B), 44–45 min (linear gradient from 90% to 80% solvent B),

Table 1
Summarization of starch-phenolic complexation process and its properties.

Phenolic type	Complexation process	Complex	Digestibility			Ref
			RDS	SDS	RS	
Polyphenol (from apple)	Starch mixed with polyphenol (5%) at various pH and gelatinized 95 °C, 20 min	V				Chou et al. (2020)
	Starch mixed with polyphenol (5%), under ultrahigh pressure (100–600 MPa) and gelatinized 95 °C 15 min	V				
Proanthocyanidin (from Chinese berry leaves)	Starch mixed with proanthocyanidins (4%) in 30% methanol, heated at 70 °C, 20 min	A + V	45.6–67.7		13.3–36.3	Zheng et al. (2021)
Gallic	Starch mixed with gallic acid (4%–50%) at 37 °C under high-speed shear (6000 rpm) for 30 min	–	47.9–75.8	7.1–15.6	12.2–45.9	Chi et al. (2019)
Gallic	Starch gelatinized at 95 °C 30 min, add gallic acid (5%–30%), high pressure homogenizer (150 MPa) for 3 times	V	72.4–95.0	1.5–9.2	1.6–29.7	Liu et al. (2019)
Gallic, Chlorogenic, Epigallocatechin- gallate, Tannic	Starch and polyphenols (10%) gelatinized at boiling water for 30 min, cooled and lyophilized	–	–	–	–	Chen, Gao, He, Yu, and Zeng (2020)
Gallic	Starch: gallic acid (1 : 0.4) was mixed at pH 4, 37 °C, high speed shearing (6000 rpm), neutralized, air dried at 40 °C	B	39.6–85.8	2.2–10.3	4.4–50.0	Chi et al. (2017)
Ferulic, Caffeic, Gallic	Starch and phenol (20:1) were mixed and dispersed in HCl solution (pH 2), oscillated overnight at 5 °C, washed, and lyophilized	–	64.4–77.4	5.4–19.9	2.3–19.2	Li et al. (2018)

45–55 min (isocratic at 80% solvent B), 55–60 min (linear gradient from 80% to 5% solvent B). The re-equilibration period of 5 min with 5% solvent B were used between individual runs. The column temperature was 38 °C. Hydroxybenzoic and hydroxycinnamic acids were detected at a 280 and 325 nm wavelength, respectively. Phenolic compounds were identified using relative retention times and UV spectra of the authentic compounds and were detected using an external standard method (Butsat & Siriamornpun, 2010). The response (area) for a known concentration of reference standard was calculated (area/concentration) to generate a calibration factor. This value was divided into the area for an unknown concentration and the result was the concentration of the unknown.

2.5. Complexation process

2.5.1. Conventional complexation process

The conventional pre-gelatinized starch–phenol complexation process was modified from Chi et al. (2018). Briefly, starch suspension (10%, w/v) (30 mL) was gelatinized in a water bath at 95 °C for 30 min with stirring. Next, crude phenolic extract calculated as total phenolic content based on gallic acid (5%, 10%, and 15%) was added to the gelatinized starch paste, stirred for 5 min, and cooled down to room temperature. The rice starch paste was washed twice with 40% ethanol and centrifuged (3000 g) for 5 min to remove uncomplexed phenol. The precipitate of rice starch–phenolic complex (termed RSP) was lyophilized, ground, sieved, and kept at 4 °C. Native rice starch was used as the negative control, and starch with gallic acid (15%) was used as the positive control.

2.5.2. Dual complexation process

The combined HMT and pre-gelatinized starch-phenolic complexation process was proposed to enhance complexation in this study. The HMT process was modified from Cham and Suwannaporn (2010). First, starch suspension (10%, w/v) (30 mL) was added with crude phenolic extract (5%) for 5 min and equilibrated at 4 °C for 24 h. The suspension was dehydrated in a hot air oven (40 °C) until the desired moisture content for HMT (25%) was achieved. The moist starch was then put in a screw-capped bottle to avoid moisture lost, and put in an oven at 110 °C for 1.5 h. After that, the starch sample underwent a second pre-gelatinization complexation process. HMT starch was suspended in water (10%, w/v)ฆ gelatinized in a 95 °C water bath, and stirred for 30 min. The second portion of crude phenolic extract (0%, 5%, 10%) was added into the starch paste to obtain a total crude phenolic at 5%, 10%, 15%, stirred for 5 min, and cooled down. The final starch paste was washed twice with 40% ethanol to remove uncomplexed phenol and centrifuged. The precipitate of HMT-rice starch-phenolic complex (termed HMT-RSP) was lyophilized, ground, sieved, and kept at 4 °C in a sealed plastic bag. Native rice starch was used as the negative control, and starch treated with gallic acid (15%) was used as the positive control.

2.6. Complexing index

All samples were accurately weighed (20 mg, db), suspended in dimethyl sulfoxide (D/4121/PB15, Fisher Scientific, Loughborough, UK) (4.0 mL), and vortexed for 2 min until completely dissolved. Solution (0.5 mL) was mixed with Folin–Ciocalteu reagent (2.0 mL) and 20% Na_2CO_3 (5.0 mL). The mixture was vigorously shaken and kept in a dark place at 25 °C for 60 min, and centrifuged at 3000 g for 1 min. The supernatant was measured at 760 nm using a UV–Vis spectrophotometer (Genesys 10S, Thermo Fisher Scientific, MA, USA). The complexing index (CI) was calculated as following equation (Meng, Ma, Sun, Wang, & Liu, 2014):

$$Complex\ \ index = \frac{Abs(sample) - Abs(control)}{Abs(control)}$$

Where, $Abs_{control}$ was absorbance of sample without phenol.

Abs_{sample} was absorbance of sample with phenol

2.7. In vitro starch digestibility

The sample was accurately weighed (0.5 g) and added with 95% ethanol (0.5 mL) and maleate buffer (17.5 mL). The capped tube was placed on a shaking water bath at 37 °C for 5 min. The α-amylase/amyloglucosidase solution (PAA 40 KU/g and AMG 17 KU/g, Megazyme, Wicklow, Ireland) (2.5 mL) was added and incubated in a shaking water bath at 37 °C. The reaction solution (1.0 mL) was removed at 20, 120, and 240 min, added into 50-mM acetic acid solution (20 mL), and then mixed thoroughly. Each solution (2 mL) was centrifuged at 13,000 rpm for 5 min, and 100-U/mL amyloglucosidase (0.1 mL) was added immediately. The solution was placed in a water bath at 50 °C for 30 min, GOPOD reagent (3.0 mL) (Megazyme, Wicklow, Ireland) was added, and then was incubated at 50 °C for 20 min. The solution was measured at absorbance 510 nm against a reagent blank. RDS, SDS, and TDS (total digestible starch) content were calculated using MegaCalc™ Excel® (K-DSTRS, Megazyme, Wicklow, Ireland).

2.8. Resistant starch (RS)

The solution (4.0 mL), which was digested for 240 min, was mixed with 95% ethanol (4.0 mL) and centrifuged (4,000 g) for 10 min. The pellet was resuspended in 50% ethanol (8 mL), 1.7-M NaOH (2 mL), and stirring for 20 min in an icee bath. The 1.2-M sodium acetate buffer (pH 3.8) (401,392, Carlo Erba, Italy) (8 mL) was added into a solution and stirred well. Amyloglucosidase (3300 U/mL, Megazyme, Wicklow, Ireland) (0.1 mL) was added immediately, incubated in a water bath at 50 °C for 30 min, and centrifuged (13,000 g) for 5 min. An aliquot (0.1 mL) was added with GOPOD reagent (3.0 mL) and incubated at 50 °C for 20 min. The solution was measured for absorbance at 510 nm against a reagent blank. RS content was calculated using MegaCalc™ Excel® (K-DSTRS, Megazyme, Wicklow, Ireland).

2.9. Fourier transform infrared spectroscopy

The FTIR spectroscopy analysis was conducted using Fourier Transform Infrared Spectroscopy (Tensor 27, Bruker Corporation, Berlin, Germany) with attenuated total reflectance accessory from 4000 to 500 cm^{-1}. For each spectrum, 32 scans using air as background were obtained at a resolution of 4 cm^{-1}. Additionally, the spectra over the range of 1200−800 cm^{-1} were automatically corrected baseline, normalized, and deconvoluted.

2.10. X-ray diffraction

The X-ray diffraction (XRD) measurement was performed using an X-ray diffractometer (D8 Advances, Bruker Corporation, Berlin, Germany). The range of the diffraction angle (2θ) was 5°–40° with a scanning speed of 10°/min and a scanning step of 0.033°. The moisture content of each sample (approximately 10%) was equilibrated at 40 °C. The relative crystallinity of the samples was calculated by the ratio of the peaks area to the total area using OriginPro 2019b software (OriginLab Corporation, MA, USA).

2.11. ^{13}C CP/MAS NMR spectroscopy

The solid-state ^{13}C CP/MAS NMR was conducted on a Bruker Avance III HD 400 Spectrometer (Bruker Corporation, Berlin, Germany) equipped with a 4 mm broadband double-resonance MAS probe. Approximately 200-mg sample was placed into the spinner and inserted into the center of magnetic field. The NMR spectrum with CP and MAS was

recorded at 400 MHz, temperature 300.3 K. A total of 1000 scans were accumulated for a spectrum with a recycle delay of 2 s. All spectra were then decomposed into several peaks through deconvolution using PeakFit version 4.12 (Sigma Plot, Systat Software, Inc., CA, USA).

2.12. Statistic analyses

All tests were conducted in triplicate, and the data were subjected to analysis of variance (ANOVA) and least significant difference test to determine the difference between means at a significance level of $p \leq 0.05$ using SPSS software package version 26 (IBM company, Chicago, Illinois, USA.).

3. Results and discussion

3.1. Complexing index

When starch was heated in water, the granules ruptured, then amylose was leached out and solubilized. Starch and phenol can form complex in two ways; an inclusion (phenol was trapped in the helix) and non-inclusion complex (phenol was trapped between helices) as shown in a schematic diagram in Fig. 1. For the inclusion complex, phenol formed a complex by hydrophobic interaction between the aromatic ring of phenol and the hydrogen bond of starch inside the amylose single helix cavity (Sun et al., 2019). The phenolic size was usually too bulky, and thus limited the capacity to enter the starch helix cavity, hence the inclusion complex could not be formed. HMT resulted in an orderly rearrangement of starch and the loose double helices in the crystalline region (Gunaratne and Hoover, 2002; Hoover & Manuel, 1996). The loose helices could allow the bulky phenol to move inside the amylose helix cavity, hence increasing V-amylose complex formation. The starch–phenolic inclusion complex could stabilize and regulate the release of phenol, which was considered a delivery system of phenol.

The complexing index (CI) of all samples increased with the higher addition of phenol (Fig. 2). This indicated excessive amylose that was ready to form a complex with phenol. Without HMT, the capability of phenol to include in the amylose helix was limited, indicated by the non-significant difference in CI regardless of different phenolic sources (within the same dosage) (Fig. 2A). By applying HMT, the CI of all starch samples was noticeably higher than the conventional process. HMT significantly promoted starch–phenolic complex formation as it generated more single helix and sites for the reactions, such as channels and hollows within the granules (Kawabata et al., 1994). CI of different phenolic sources then showed significant differences in complex formation (Fig. 2B). The highest CI was found in Riceberry, followed by KDML and milky stage rice within the same dosage. The dual complexation process using 15% Riceberry extract was double (5.03%, 6.80%, and 10.17%) the conventional process (1.97%, 3.2%, and 5.14%) at dosage 5%, 10%, and 15%, respectively (Fig. 2). The effect of phenolic composition in the crude extract was further investigated in Section 3.2.

3.2. Total phenolic content and its characterization

According to the previous result in section 3.1, the content of starch–phenolic complex is depended on total phenolic content (TPC), type of phenol, and inclusion process. The interaction between starch and polyphenol mainly depended on the molecular size of the phenolic compound (Zhu, 2015). Crude phenolic extract from rice bran of Riceberry had the highest TPC and hydroxycinnamic acid, especially ferulic acid (Table 2). The main phenolic acid in Riceberry was protocatechuic, vanillic, and ferulic acid, whereas ferulic acid and vanillic acid were the main phenolic acid found in white rice and young rice, respectively (Table 2). Hydroxycinnamic acids, such as ferulic, *p*-coumaric, caffeic, and sinapic acids, effectively inhibited α-amylase activity. Hydroxycinnamic acid consists of a C═C double bond, which conjugates with the carbonyl group and binds with the enzyme's active site (Sun et al., 2019).

3.3. In vitro starch digestibility

The complexation of starch with phenol by either inclusion or non-inclusion could decrease starch digestibility. The starch–phenolic complex reduced starch digestibility in two aspects, the inhibition of phenol on digestive enzymes and the starch structure (V-type), which resisted digestion. However, after ingestion, only 5%–10% of phenol was absorbed in the small intestine, the remaining was transformed, absorbed, and utilized by intestinal microflora in the large intestine or discharged with feces (Cardona, Andrés-Lacueva, Tulipani, Tinahones, & Queipo-Ortuño, 2013). The V-amylose inclusion complex showed slowly or resistance to enzymatic digestion, and was defined as resistant starch type 5 (RS 5) (Cohen, Schwartz, Peri, & Shimoni, 2011). Moreover, phenol itself acted as a competitive inhibitor for digestive enzymes. The aromatic ring of phenolic compound competed with starch to form a hydrophobic interaction with tryptophan residue of α-amylase (Sun et al., 2019). The dual complexation process using 15% Riceberry extract (HMT-RSP-Riceberry) showed much lower RDS (77.19%), higher SDS (7.05%) and RS (15.76%) than the conventional process (90.27, 3.48, and 6.25%), and even better than the positive control (87.59, 5.27, and 7.14%, respectively) (Table 3). Dual complexation using crude Riceberry extract obviously improved rice starch digestibility, as HMT promoted more single helix and loosened double helices structure, as previously mentioned.

3.4. Fourier-transform infrared spectrometry

The FTIR spectra of native starch, RSP, and HMT-RSP complex had similar functional groups but with different peak intensities (Fig. 3).

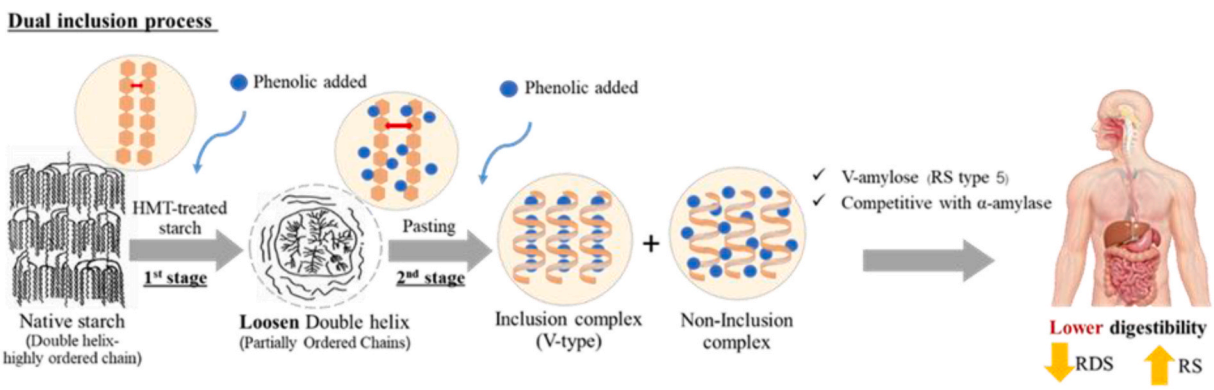

Fig. 1. Hypothesis and schematic of the formation of starch–phenol complex under a dual inclusion complexation and its ability to control digestibility.

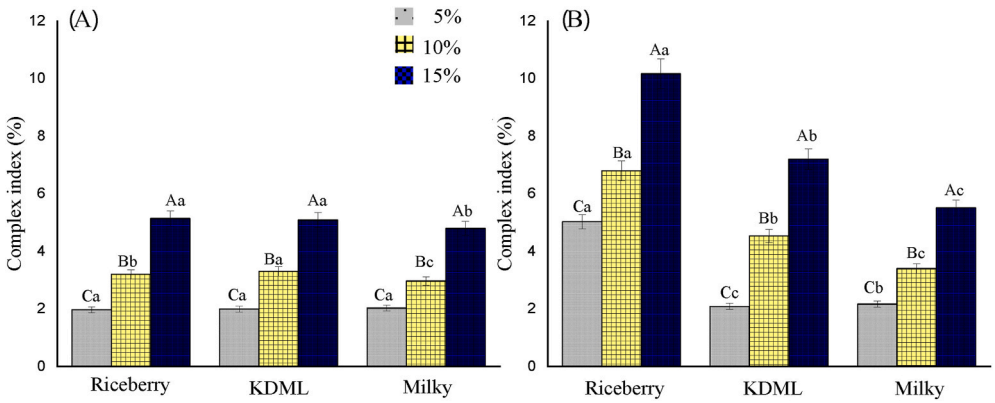

Fig. 2. Complexing index of rice starch phenolic complex using (A) Conventional (B) Dual complexation process.
[A–C] mean value with different superscript indicated a significant difference ($p \leq 0.05$) among different dosages.
[a–c] mean value with different superscripts indicated a significant difference ($p \leq 0.05$) among different phenolic types.

Table 2
Total phenolic content and profile in the various crude phenolic extracts of rice.

Phenolic profile	Crude phenolic extract (μg/g)		
	Riceberry	KDML	Milky
Total phenolic content	3374.00 ± 3.46[a]	2010.00 ± 2.65[b]	724.00 ± 1.73[c]
Hydroxycinnamic acid			
Ferulic	50.23 ± 6.18[a]	35.84 ± 0.8[b]	1.59 ± 0.39[c]
p-Coumaric	9.00 ± 0.93[a]	5.34 ± 0.16[b]	1.70 ± 0.54[c]
Sinapic	6.67 ± 0.20[a]	3.73 ± 2.58[b]	3.67 ± 0.64[b]
Caffeic	5.90 ± 0.21[a]	5.40 ± 1.94[b]	2.69 ± 0.28[c]
Hydroxybenzoic acid			
Protocatechuic	80.56 ± 2.53[a]	7.99 ± 2.10[c]	18.13 ± 0.27[b]
Vanillic	50.80 ± 2.53[b]	12.30 ± 8.76[c]	53.47 ± 1.87[a]
Gallic acid	ND	ND	1.75 ± 1.03

[a-c] mean value in row with different superscript indicated a significant difference ($p \leq 0.05$).
ND: No-detection.

Table 3
RDS, SDS, and RS contents of rice starch–phenolic complex.

Starch–phenolic complex	Starch digestibility		
	RDS (%)	SDS (%)	RS (%)
Conventional complexation process			
Native starch (–ve control)	95.93 ± 0.18[a]	1.50 ± 0.05[h]	2.57 ± 0.05[j]
RSP-15%GA (+ve control)	87.59 ± 0.44[d]	5.27 ± 0.05[b]	7.14 ± 0.02[f]
RSP-KDML	93.07 ± 0.39[b]	2.86 ± 0.07[d]	4.07 ± 0.05[i]
RSP-Riceberry	90.27 ± 0.18[c]	3.48 ± 0.08[c]	6.25 ± 0.03[g]
RSP-Milky	93.32 ± 0.21[b]	1.77 ± 0.03[g]	4.91 ± 0.03[h]
Dual complexation process			
HMT Starch (-ve control)	90.06 ± 0.19[c]	2.43 ± 0.08[e]	7.51 ± 0.06[e]
HMT-RSP-GA (+ve control)	84.93 ± 0.18[f]	2.11 ± 0.03[f]	12.96 ± 0.03[b]
HMT-RSP-KDML	88.18 ± 0.17[d]	1.23 ± 0.04[i]	10.59 ± 0.04[d]
HMT-RSP-Riceberry	77.19 ± 0.14[g]	7.05 ± 0.07[a]	15.76 ± 0.04[a]
HMT-RSP-Milky	86.41 ± 0.26[e]	1.75 ± 0.05[g]	11.84 ± 0.02[c]

[a-j] mean value in column with different superscript indicated a significant difference ($p \leq 0.05$).

HMT did not affect functional groups but decreased the IR absorption peak at 1200–1000 cm^{-1} (Fig. 3C). The peak intensity of HMT-RSP was lower because the interaction between phenol and starch destroyed hydrogen bonds and reduced orderly starch structure (Chi et al., 2019; Lv et al., 2020). The C═O stretching vibrations at 1697 cm^{-1}, and strong signals at 3276 cm^{-1} and 3520 cm^{-1} were assigned to *C*–H stretching vibration of unsaturated carbon and phenol hydroxyl stretching vibrations that showed the strong signals of phenolic compounds (Liu et al., 2019). The IR absorbance at 1045 and 1022 cm^{-1} was related to the crystalline/ordered and amorphous starch structure, respectively. Therefore, the ratio of 1045/1022 cm^{-1} was calculated to identify the difference in the molecular structure of starch and its complex (van Soest, de Wit, Tournois, & Vliegenthart, 1994). After HMT, the ratio of 1045/1022 cm^{-1} increased, indicating a higher crystalline structure (Fig. 3D).

3.5. *X-ray diffraction (XRD)*

All starch samples exhibited a V-type diffraction pattern with characteristic peaks (2θ) at 13.0° and 19.8°. However, more distinct peaks were seen in samples with starch–phenolic complex than native starch paste and HMT starch paste (Fig. 4). A single-helical amylose–phenolic complex or V-type starch had a high degree of order resulted in the increase in crystallinity (from 19.82% to 31.54%), and the decrease in amorphous (from 80.18% to 68.46%) (Table 4) (Cohen et al., 2011). After dual complexation, HMT-RSP-Riceberry showed the highest V-type (30.79%) compared with native starch paste (14.49%) and HMT starch paste (20.58%) (Table 4). This result agreed with the result of *in vitro* digestibility in section 3.3.

3.6. *^{13}C CP/MAS NMR spectroscopy*

The ^{13}C CP/MAS NMR spectra were used to identify the short-range ordered molecular structure of starch which were single and double helices. The signal resonance for C_1, C_4, and C_6 were at approximately 94–105, 81–83, and 59–65 ppm regions. Peaks for C_2, C_3, and C_5 were at approximately 66–74 ppm regions. Within the C_1 region, peaks at approximately 99–102 ppm were a characteristic of V-type single helix. The C_4 resonance peak at approximately 81–82 ppm and peak at 103.2 ppm were related to amorphous starch and were associated with the junction points of amylopectin double helices (Liu et al., 2019). The detailed alteration of the amorphous and helical conformations was shown in Table 5.

The double helices fraction of starch was noticeably decreased after complexation, especially with the dual complexation (9.77%–4.36%). As the starch double helices fraction decreased, the single helix fraction surged from 4.26% in native starch to 24.72% in the conventional process and 30.73% in the dual complexation process. The result agreed well with the amorphous fraction, which reduced after complexation from 85.97% in native to 67.35% in conventional process and 64.91% in dual complexation process. The reduction in amorphous of the dual complexation process was not pronounced as the increase in V-type crystalline as HMT itself also increased amorphous area in the semi-crystalline lamella of starch (Gunaratne & Hoover, 2002). HMT promoted more loose helices that ease the interaction between starch and phenolic compounds (Fig. 1), hence increasing more complexation in both inclusion and non-inclusion mechanisms. When a single helix

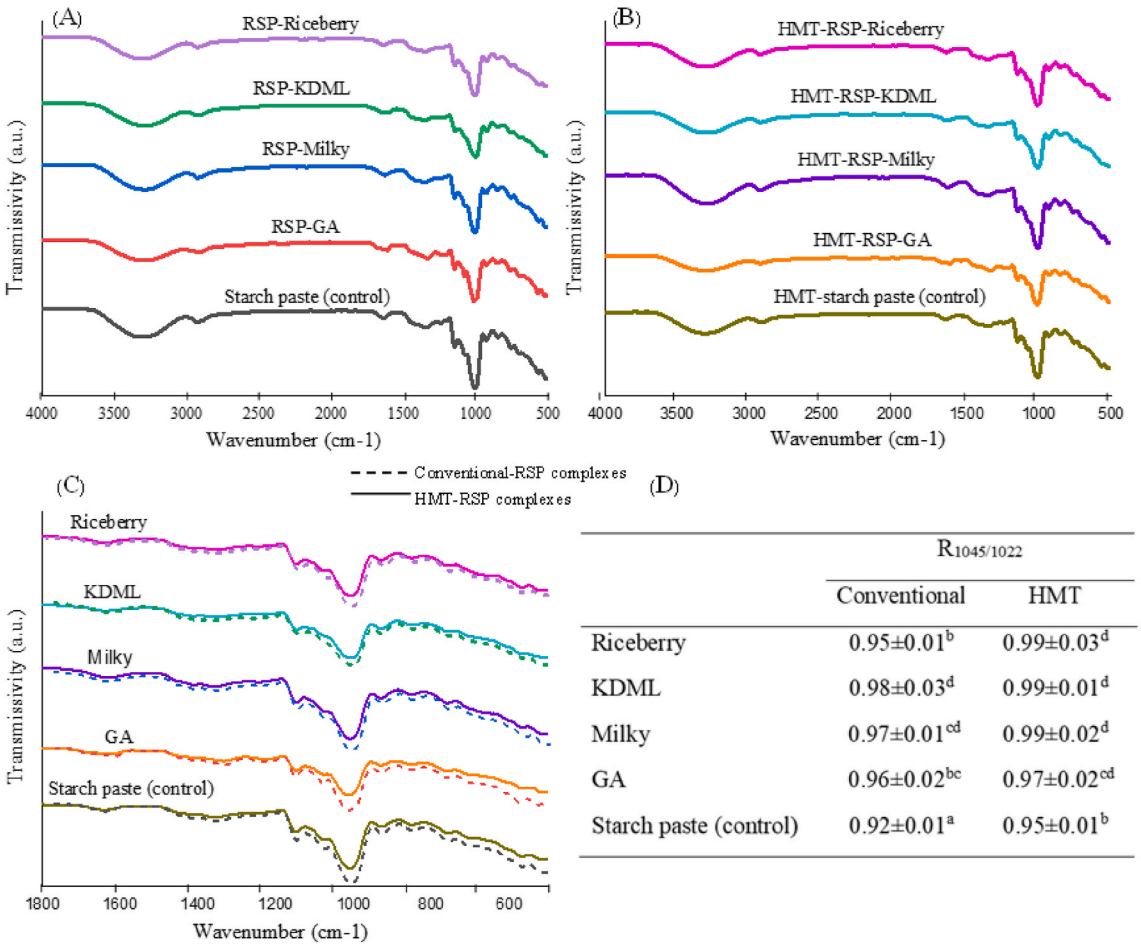

	$R_{1045/1022}$	
	Conventional	HMT
Riceberry	0.95±0.01[b]	0.99±0.03[d]
KDML	0.98±0.03[d]	0.99±0.01[d]
Milky	0.97±0.01[cd]	0.99±0.02[d]
GA	0.96±0.02[bc]	0.97±0.02[cd]
Starch paste (control)	0.92±0.01[a]	0.95±0.01[b]

Fig. 3. FTIR spectra of (A) RSP (B) HMT-RSP (C) overlay spectra of RSP and HMT-RSP (D) ratio of IR absorbance at 1045 cm^{-1} and 1022 cm^{-1}.

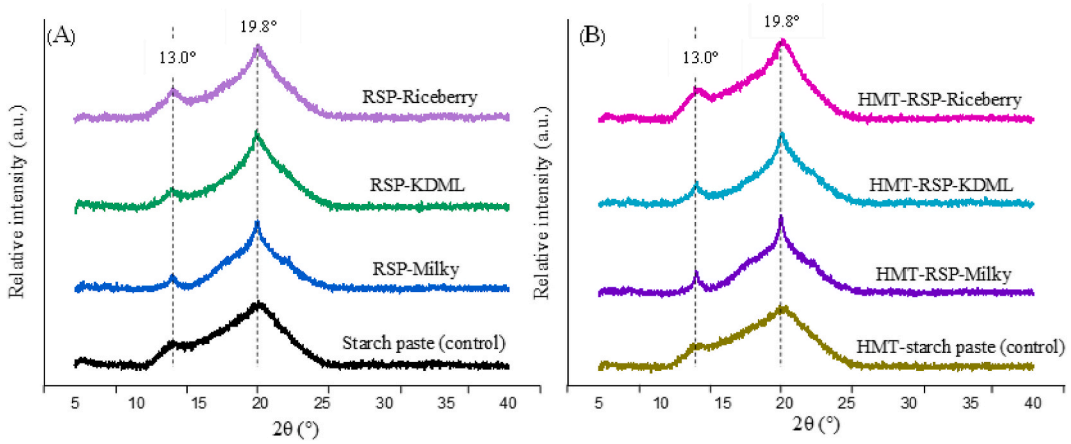

Fig. 4. X-ray diffraction pattern of (A) RSP (B) HMT-RSP.

structure was present in the system, it tended to form a densely packed domain which decreased the proportion of amorphous. These results were consistent with the result of XRD, which verified the formation of V-type structure.

4. Conclusion

The ability of starch to form amylose–phenolic complex was depended on the amylose content of starch, type and content of phenol, and how to incorporate these phenol into the helical structure of amylose. Phenolic extract from Riceberry rice showed the highest ability to form complex with amylose. The dual process using HMT and pre-gelatinization was an effective method to obtain V-amylose of rice starch-phenolic complex. The molecular rearrangement that occurred during HMT promoted a looser starch structure and increased the interaction between starch and phenol to form single helix inclusion complex or V-type amylose. Thus, RDS was transformed into SDS and RS. The inclusion of phenol into the cavity of single amylose helix or trapped between these helical structures could improve starch digestibility with potential application in healthy foods. This

Table 4
The relative amorphous, crystallinity, and V-amylose of rice starch-phenolic complex from conventional and dual complexation process.

	% V-amylose	% Amorphous	% Crystallinity
Conventional complexation process			
RSP-Riceberry	25.79 ± 0.11^{b}	72.06 ± 0.09^{f}	27.94 ± 0.04^{b}
RSP-KDML	23.30 ± 0.13^{d}	72.15 ± 0.09^{f}	27.85 ± 0.06^{b}
RSP-Milky	17.61 ± 0.07^{g}	79.60 ± 0.07^{b}	20.40 ± 0.05^{f}
Starch paste (control)	14.49 ± 0.29^{h}	80.18 ± 0.06^{a}	19.82 ± 0.07^{g}
Dual complexation process			
HMT-RSP-Riceberry	30.79 ± 0.09^{a}	68.46 ± 0.06^{g}	31.54 ± 0.04^{a}
HMT-RSP-KDML	25.41 ± 0.06^{c}	72.70 ± 0.03^{e}	27.30 ± 0.04^{c}
HMT-RSP-Milky	21.60 ± 0.05^{e}	76.54 ± 0.04^{d}	23.46 ± 0.06^{d}
HMT-starch paste (control)	20.58 ± 0.08^{f}	76.86 ± 0.06^{c}	23.14 ± 0.06^{e}

$^{a\text{-}h}$ mean value in column with different superscript indicated a significant difference ($p \leq 0.05$).

Table 5
The ^{13}C CP/MAS NMR spectra showed peak position and relative proportion of the complexes' helix conformation.

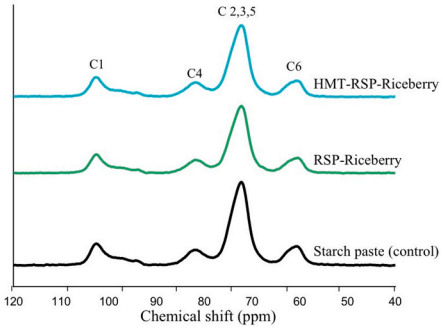

Sample	Relative proportion (%)			Peak position (ppm)	
	double helices	single helix	amorphous	C_1	C_4
Starch (control)	9.77 ± 0.27^{a}	4.26 ± 0.31^{c}	85.97 ± 0.27^{a}	94.9, 98.2, 102.5	81.5
RSP-Riceberry	7.93 ± 0.27^{b}	24.72 ± 0.38^{b}	67.35 ± 0.49^{b}	94.9, 98.9, 102.6	81.5
HMT-RSP-Riceberry	4.36 ± 0.35^{c}	30.73 ± 0.19^{a}	64.91 ± 0.23^{c}	94.4, 99.7, 102.6	81.4

$^{a\text{-}c}$ Mean values in column with different subscripts indicate a significant difference ($p \leq 0.05$).
Note: The complexation was conducted at 15% crude phenol from Riceberry rice bran.

complexation process was a simple and no chemical used technique. Moreover, it was applicable in terms of reasonable amount of phenol used and no undesirable taste, which made it possible to apply in large scale production either with rice starch or rice grain.

Data availability

Data will be made available on request.

Acknowledgments

This research and innovation activity is funded by the National Research Council of Thailand (NRCT) and Kasetsart University Research and Development (KURDI), grant number FF(KU) 26.66.

References

Butsat, S., & Siriamornpun, S. (2010). Antioxidant capacities and phenolic compounds of the husk, bran and endosperm of Thai rice. *Food Chemistry, 119*(2), 606–613. https://doi.org/10.1016/j.foodchem.2009.07.001

Cardona, F., Andrés-Lacueva, C., Tulipani, S., Tinahones, F. J., & Queipo-Ortuño, M. I. (2013). Benefits of polyphenols on gut microbiota and implications in human health. *Journal of Nutritional Biochemistry, 24*(8), 1415–1422. https://doi.org/10.1016/j.jnutbio.2013.05.001

Cham, S., & Suwannaporn, P. (2010). Effect of hydrothermal treatment of rice flour on various rice noodles quality. *Journal of Cereal Science, 51*(3), 284–291. https://doi.org/10.1016/j.jcs.2010.01.002

Chen, N., Gao, H. X., He, Q., Yu, Z. L., & Zeng, W. C. (2020). Interaction and action mechanism of starch with different phenolic compounds. *International Journal of Food Sciences & Nutrition, 71*(6), 726–737. https://doi.org/10.1080/09637486.2020.1722074

Chen, P. N., Kuo, W. H., Chiang, C. L., Chiou, H. L., Hsieh, Y. S., & Chu, S. C. (2006). Black rice anthocyanins inhibit cancer cells invasion via repressions of MMPs and u-PA expression. *Chemico-Biological Interactions, 163*(3), 218–229. https://doi.org/10.1016/j.cbi.2006.08.003

Chi, C., Li, X., Feng, T., Zeng, X., Chen, L., & Li, L. (2018). Improvement in nutritional attributes of rice starch with dodecyl gallate complexation: A molecular dynamic simulation and *in vitro* study. *Journal of Agricultural and Food Chemistry, 66*(35), 9282–9290. https://doi.org/10.1021/acs.jafc.8b02121

Chi, C., Li, X., Zhang, Y., Chen, L., Li, L., & Wang, Z. (2017). Digestibility and supramolecular structural changes of maize starch by non-covalent interactions with gallic acid. *Food & Function, 8*(2), 720–730. https://doi.org/10.1039/c6fo01468b

Chi, C., Li, X., Zhang, Y., Chen, L., Xie, F., Li, L., et al. (2019). Modulating the *in vitro* digestibility and predicted glycemic index of rice starch gels by complexation with gallic acid. *Food Hydrocolloids, 89*, 821–828. https://doi.org/10.1016/j.foodhyd.2018.11.016

Chou, S., Li, B., Tan, H., Zhang, W., Zang, Z., Cui, H., et al. (2020). The effect of pH on the chemical and structural interactions between apple polyphenol and starch derived from rice and maize. *Food Sciences and Nutrition, 8*(9), 5026–5035. https://doi.org/10.1002/fsn3.1800

Cohen, R., Schwartz, B., Peri, I., & Shimoni, E. (2011). Improving bioavailability and stability of genistein by complexation with high-amylose corn starch. *Journal of Agricultural and Food Chemistry, 59*(14), 7932–7938. https://doi.org/10.1021/jf2013277

Gao, S., Liu, H., Sun, L., Cao, J., Yang, J., Lu, M., et al. (2021). Rheological, thermal and *in vitro* digestibility properties on complex of plasma modified Tartary buckwheat starches with quercetin. *Food Hydrocolloids, 110*. https://doi.org/10.1016/j.foodhyd.2020.106209

Gunaratne, A., & Hoover, R. (2002). Effect of heat–moisture treatment on the structure and physicochemical properties of tuber and root starches. *Carbohydrate Polymers, 49*(4), 425–437. https://doi.org/10.1016/S0144-8617(01)00354-X

Guo, Z., Zhao, B., Chen, J., Chen, L., & Zheng, B. (2019). Insight into the characterization and digestion of lotus seed starch-tea polyphenol complexes prepared under high hydrostatic pressure. *Food Chemistry, 297*, Article 124992. https://doi.org/10.1016/j.foodchem.2019.124992

Han, M., Bao, W., Wu, Y., & Ouyang, J. (2020). Insights into the effects of caffeic acid and amylose on *in vitro* digestibility of maize starch-caffeic acid complex. *International Journal of Biological Macromolecules, 162*, 922–930. https://doi.org/10.1016/j.ijbiomac.2020.06.200

Hoover, R., & Manuel, H. (1996). The effect of heat–moisture treatment on the structure and physicochemical properties of normal maize, waxy maize, dull waxy maize and amylomaize V starches. *Journal of Cereal Science, 23*(2), 153–162. https://doi.org/10.1006/jcrs.1996.0015

Kawabata, A., Takase, N., Miyoshi, E., Sawayama, S., Kimura, T., & Kudo, K. (1994). Microscopic observation and X-ray diffractometry of heat/moisture-treated starch granules. *Starch - Stärke, 46*(12), 463–469. https://doi.org/10.1002/star.19940461204

Kwon, O., Eck, P., Chen, S., Corpe, C. P., Lee, J. H., Kruhlak, M., et al. (2007). Inhibition of the intestinal glucose transporter GLUT2 by flavonoids. *Federation of American Societies for Experimental Biology Journal, 21*(2), 366–377. https://doi.org/10.1096/fj.06-6620com

Liu, Y., Chen, L., Xu, H., Liang, Y., & Zheng, B. (2019). Understanding the digestibility of rice starch-gallic acid complexes formed by high pressure homogenization. *International Journal of Biological Macromolecules, 134*, 856–863. https://doi.org/10.1016/j.ijbiomac.2019.05.083

Liu, Q., & Yao, H. (2007). Antioxidant activities of barley seeds extracts. *Food Chemistry, 102*(3), 732–737. https://doi.org/10.1016/j.foodchem.2006.06.051

Li, K., Yao, F., Du, J., Deng, X., & Li, C. (2018). Persimmon tannin decreased the glycemic response through decreasing the digestibility of starch and inhibiting α-amylase, α-glucosidase, and intestinal glucose uptake. *Journal of Agricultural and Food Chemistry, 66*(7), 1629–1637. https://doi.org/10.1021/acs.jafc.7b05833

Lv, Y., Li, M., Pan, J., Zhang, S., Jiang, Y., Liu, J., et al. (2020). Interactions between tea products and wheat starch during retrogradation. *Food Bioscience, 34*. https://doi.org/10.1016/j.fbio.2019.100523

Meng, S., Ma, Y., Sun, D., Wang, L., & Liu, T. (2014). Properties of starch-palmitic acid complexes prepared by high pressure homogenization. *Journal of Cereal Science, 59*, 25–32. https://doi.org/10.1016/j.jcs.2013.10.012

Obiro, W. C., Sinha Ray, S., & Emmambux, M. (2012). V-amylose structural characteristics, methods of preparation, significance, and potential applications. *Food Reviews International, 28*(4), 412–438. https://doi.org/10.1080/87559129.2012.660718

Pantoa, T., Baricevic-Jones, I., Suwannaporn, P., Kadowaki, M., Kubota, M., Roytrakul, S., et al. (2020). Young rice protein as a new source of low allergenic plant-base protein. *Journal of Cereal Science, 93*, Article 102970. https://doi.org/10.1016/j.jcs.2020.102970

Ratseewo, J., Warren, F. J., & Siriamornpun, S. (2019). The influence of starch structure and anthocyanin content on the digestibility of Thai pigmented rice. *Food Chemistry, 298*, Article 124949. https://doi.org/10.1016/j.foodchem.2019.06.016

van Soest, J. J. G., de Wit, D., Tournois, H., & Vliegenthart, J. F. G. (1994). Retrogradation of potato starch as studied by Fourier transform infrared spectroscopy. *Starch - Stärke, 46*(12), 453–457. https://doi.org/10.1002/star.19940461202

Sun, L., Warren, F. J., & Gidley, M. J. (2019). Natural products for glycaemic control: Polyphenols as inhibitors of alphaα-amylase. *Trends in Food Science & Technology, 91*, 262–273. https://doi.org/10.1016/j.tifs.2019.07.009

Wang, H. G., Gao, J. M., Liu, W., Zhang, M., & Guo, M. (2016). Recovery of metal-doped zinc ferrite from zinc-containing electric arc furnace dust: Process development and examination of elemental migration. *Hydrometallurgy, 166*, 1–8. https://doi.org/10.1016/j.hydromet.2016.08.004

Zhao, B., Sun, S., Lin, H., Chen, L., Qin, S., Wu, W., et al. (2019a). Physicochemical properties and digestion of the lotus seed starch-green tea polyphenol complex under ultrasound-microwave synergistic interaction. *Ultrasonics Sonochemistry, 52*, 50–61. https://doi.org/10.1016/j.ultsonch.2018.11.001

Zhao, B., Wang, B., Zheng, B., Chen, L., & Guo, Z. (2019b). Effects and mechanism of high-pressure homogenization on the characterization and digestion behavior of lotus seed starch–green tea polyphenol complexes. *Journal of Functional Foods, 57*, 173–181. https://doi.org/10.1016/j.jff.2019.04.016

Zheng, Y., Tian, J., Kong, X., Wu, D., Chen, S., Liu, D., et al. (2021). Proanthocyanidins from Chinese berry leaves modified the physicochemical properties and digestive characteristic of rice starch. *Food Chemistry, 335*, Article 127666. https://doi.org/10.1016/j.foodchem.2020.127666

Zhu, F. (2015). Interactions between starch and phenolic compound. *Trends in Food Science & Technology, 43*(2), 129–143. https://doi.org/10.1016/j.tifs.2015.02.003